PAPER

The bead on a rotating hoop revisited: an unexpected resonance

IOP Publishing European Journal of Physics
Eur. J. Phys. **38** (2017) 015005 (13pp) doi:10.1088/0143-0807/38/1/015005

The bead on a rotating hoop revisited: an unexpected resonance

Lisandro A Raviola, Maximiliano E Véliz, Horacio D Salomone, Néstor A Olivieri and Eduardo E Rodríguez

Instituto de Industria, Universidad Nacional de General Sarmiento. Juan María Gutiérrez 1150, (B1613GSX) Los Polvorines, Buenos Aires, Argentina

E-mail: lraviola@ungs.edu.ar

Received 30 September 2016
Accepted for publication 3 November 2016
Published 6 December 2016

Abstract

The bead on a rotating hoop is a typical problem in mechanics, frequently posed to junior science and engineering students in basic physics courses. Although this system has a rich dynamics, it is usually not analysed beyond the point particle approximation in undergraduate textbooks, nor empirically investigated. Advanced textbooks show the existence of bifurcations owing to the system's nonlinear nature, and some papers demonstrate, from a theoretical standpoint, its points of contact with phase transition phenomena. However, scarce experimental research has been conducted to better understand its behaviour. We show in this paper that a minor modification to the problem leads to appealing consequences that can be studied both theoretically and empirically with the basic conceptual tools and experimental skills available to junior students. In particular, we go beyond the point particle approximation by treating the bead as a rigid spherical body, and explore the effect of a slightly non-vertical hoop's rotation axis that gives rise to a resonant behaviour not considered in previous works. This study can be accomplished by means of digital video and open source software. The experience can motivate an engaging laboratory project by integrating standard curriculum topics, data analysis and experimental exploration.

Keywords: rigid body, bifurcation, digital video, experimentation, resonance

(Some figures may appear in colour only in the online journal)

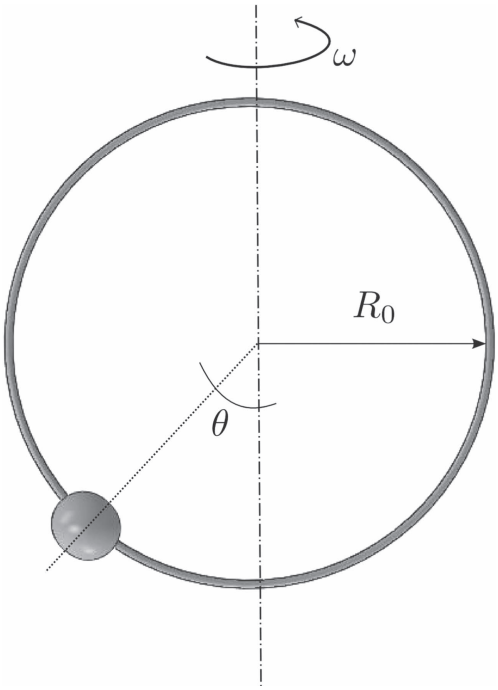

Figure 1. Schematic representation of the bead-on-a-hoop problem.

1. Introduction

The teaching of mechanics for physics and engineering students in the first university years has been historically a pedagogic challenge. It is usually the earliest exposure to the foundations of physics that students face, which presents to them a number of new concepts and technical difficulties [1]. In this context, students are supposed to learn Newton's laws for point particles and systems, the ideas of work and mechanical energy, momentum and energy conservation, simple harmonic motion and elementary rigid body dynamics [2, 3]. The difficulties are generally overcome by applying the fundamental physical laws and principles to the analysis of simplified 'toy' models, which show the essential features of basic phenomena without the technical complexities that would hinder the understanding of the relevant concepts. In parallel with the analytical development, students usually participate in demonstrations and laboratory activities with the aim of supporting the theoretical development with empirical evidence. Standard demonstrations are pretty straightforward and explore models that can be solved analytically, directly or by means of reasonable approximations. Within this class we find free-falling bodies and projectiles, carts or disks moving over inclined planes, planar pendulums, and spring-mass oscillators, among others [4, 5]. However, many textbook problems are not investigated experimentally nor connected with laboratory activities, giving the students the erroneous impression that they are just 'ideal' pencil-and-paper exercises outside the scope of empirical enquiry. This can lead to low levels of student motivation and engagement, and could produce a distorted perception about the scientific activity. In the past, this unfortunate situation was justified by the practical complexity of the needed experiments and the lack of adequate experimental resources. Nevertheless, the rapid development of information technology in recent years has brought to physics teachers and

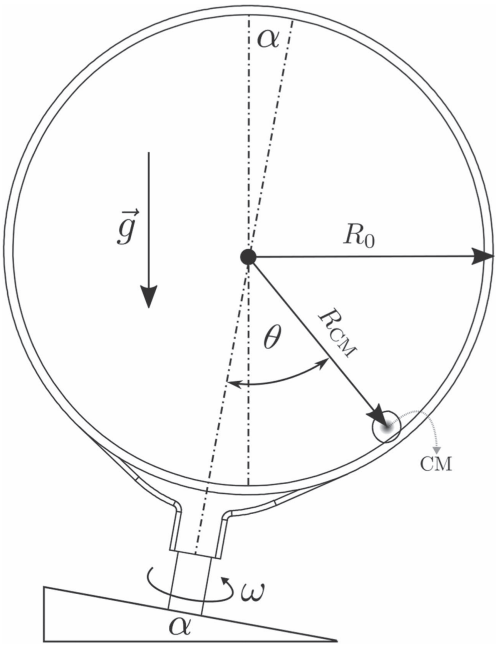

Figure 2. Actual system configuration and relevant parameters.

students a whole new world of experimental and didactic tools that can be applied with profit to previously inaccessible situations. Besides the now ubiquitous (and usually expensive) computer-based data acquisition devices, emerging powerful technologies like digital video [6], 3D printing [7] and a variety of sensors embedded in cheap mobile devices [8] are entering the educational arena at a steady pace. On the other hand, free and open source software for scientific computing and data analysis is reaching maturity and accessibility [9]. With these new tools at hand, many old problems can be resignified and the aforementioned disconnection between theory and experiment can be overcome in many important cases.

As an example of this approach, we develop in the present article an investigation of the traditional problem of a bead constrained to move on a uniformly rotating hoop—schematically depicted in figure 1—that appears in many physics textbooks in the context of rotational motion [2, 3] and Lagrangian dynamics [10]. An interesting aspect, generally not discussed in elementary courses, is the existence of a bifurcation due to the nonlinear nature of the system, which is analysed from a theoretical point of view in specialised dynamics textbooks like [11].

The problem has appeared in many studies that discuss the analogy between this system (or some variant) and phase transition phenomena of statistical mechanics, but they are exclusively theoretical, lacking experimental development [12–16]. On the other hand, Mancuso [17, 18] shows empirically—but only in a qualitative way—the existence of a bifurcation, using a manually controlled experimental device (the Groove Tube). The system is also experimentally investigated in the context of a nonlinear dynamics course using traditional (analog) video techniques, obtaining quantitatively the bifurcation diagram [19]. However, in all these references the authors remain within the limits of the point-particle approximation—even in cases when the actual 'bead' is a sphere that rolls over the interior surface of the hoop—and the experimental side of the question is not explored exhaustively.

In this paper, we report the development of a more thorough experimental approach to study the dynamics of a bead on a rotating hoop. In addition, we present an analysis to improve the existing theoretical treatment while considering the bead as a rigid rolling sphere. Likewise, we introduce the original variant of taking into account the effects of a slightly non-vertical rotation axis, which leads to a resonant behaviour not identified in previous works. Using digital video and open source software, we show that all these features are amenable to an approach involving both theory and experiments that is suitable for junior students.

2. Theoretical considerations

We begin by paraphrasing the traditional textbook problem, which reads as follows [2, 3]:

> 'A small bead of mass m can slide with a slight amount of friction on a circular hoop that is in a vertical plane and has a radius R_0. The hoop rotates at a constant rate ω about a vertical diameter. Find the angle θ at which the bead is in vertical equilibrium.'

The situation is schematically represented in figure 1 and analysed in section 2.1. The analysis summarises the physics behind the presence of a bifurcation [11] and embraces the case of a rotating hoop around a slightly tilted axis to discover a parameter-dependent resonance present in this system. In addition, in section 2.2, we develop the theoretical tools needed to analyse the case of a real rigid, spherical bead over the hoop and again with the interesting variation of a non-vertical rotation axis, as depicted in figure 2.

2.1. Point-like bead and tilted axis of rotation: bifurcations and resonance

Although we will experimentally study the rolling motion of a rigid sphere over a groove in the interior side of the rotating hoop, for comparison purposes we first obtain the equation of motion (EOM) for a point-like bead. This treatment comprises the case of a non-vertical rotating axis, which gives rise to some resonance phenomena not previously identified.

The Lagrangian approach is straightforward. The kinetic energy T reads

$$T = \frac{1}{2} m R_0^2 (\dot{\theta}^2 + \sin^2\theta\ \omega^2). \tag{1}$$

The potential energy V, as can be deduced by looking at figure 2 (although considering a point-like bead), is given by

$$V = -mgR_0(\cos\alpha\cos\theta + \sin\alpha\cos(\omega t)\sin\theta), \tag{2}$$

where θ is the angle measured from the bottom of the hoop with respect to the direction of the rotation axis and α is the angle formed between the rotation axis and the vertical direction. We suppose the presence of a friction force proportional to the bead velocity [20]

$$\vec{F} = -b\vec{v} \tag{3}$$

which leads to the generalised force

$$Q_\theta = -bR_0^2\dot{\theta}. \tag{4}$$

Inserting the previous expressions into the Lagrangian $\mathcal{L} = T - V$ and operating in the usual form we get the following EOM

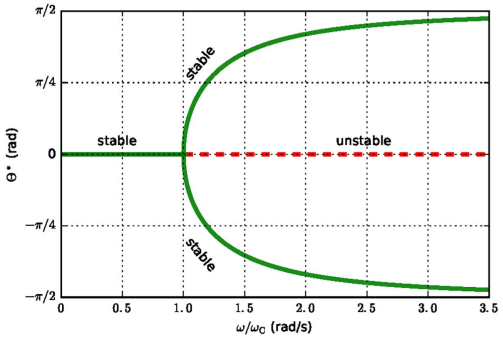

Figure 3. Bifurcation diagram: behaviour of equilibrium angle θ^* as a function of the normalised angular velocity ω/ω_C for a hoop with radius $R_0 = 0.183$ m.

$$\ddot{\theta} + \frac{b}{m}\,\dot{\theta} + \left(\cos\alpha\frac{g}{R_0} - \omega^2\cos\theta\right)\sin\theta = \frac{g}{R_0}\sin\alpha\cos(\omega t)\cos\theta. \tag{5}$$

This equation includes a term with a factor that varies periodically with time. If the tilt angle α is small, the previous EOM can be simplified to

$$\ddot{\theta} + \frac{b}{m}\,\dot{\theta} + \left(\frac{g}{R_0} - \omega^2\cos\theta\right)\sin\theta = \frac{g}{R_0}\alpha\cos(\omega t)\cos\theta. \tag{6}$$

For the particular case $\alpha = 0$ (vertical rotation axis), the forcing term disappears and the bead settles, by virtue of the friction term, at the equilibrium positions $\theta = \theta^*$ associated to the condition $\dot{\theta} = \ddot{\theta} = 0$, whence

$$\sin\theta^* = 0 \Rightarrow \theta^* = 0,\ \pi$$

or

$$\cos\theta^* = \frac{g}{\omega^2 R_0} \Rightarrow \theta^* = \arccos\left(\frac{g}{\omega^2 R_0}\right). \tag{7}$$

However, the last equilibrium configuration exists only if

$$\omega \geqslant \sqrt{\frac{g}{R_0}} = \omega_C \tag{8}$$

i.e, if the angular velocity of the hoop ω is greater than a *critical angular velocity* ω_C. Below the critical velocity ($\omega < \omega_C$), the θ, $\dot{\theta} = 0$ configuration is a *stable* equilibrium. In fact, if θ, $\dot{\theta} \ll 1$ then $\ddot{\theta} \approx \theta(\omega^2 - \omega_C^2) < 0$. Consequently, the natural angular frequency for small oscillations of the bead about this stable equilibrium position depends on ω and is given by

$$\omega_0 = \sqrt{\omega_C^2 - \omega^2}\,. \tag{9}$$

When $\omega > \omega_C$, the phase space point $(\theta, \dot{\theta}) = (0, 0)$ turns into an *unstable* equilibrium. On the other hand, linearising the EOM about $\dot{\theta} = 0$, $\theta = \arccos(\omega_C^2/\omega^2) = \theta^*$ we obtain $\ddot{\theta} \approx -\omega^2\sin^2\theta^*(\theta - \theta^*)$, whereby the equilibrium position $\theta = \theta^*$ is always stable. This behaviour of the stability points as the parameter ω varies, represented in figure 3, is called a *supercritial pitchfork bifurcation* about the critical value ω_C. This is the behaviour analysed in [11–14, 17, 19] in the case $\alpha = 0$.

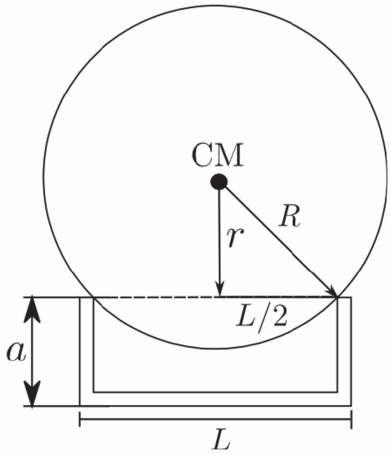

Figure 4. Transversal section of the groove where the rigid sphere rolls.

Furthermore, considering small angles θ in (6) we obtain the following EOM

$$\ddot{\theta} + \frac{b}{m}\dot{\theta} + \left(\frac{g}{R_0} - \omega^2\right)\theta = \frac{g}{R_0}\alpha\cos(\omega t) \tag{10}$$

which corresponds to a forced harmonic oscillator when $\omega < \omega_C = \sqrt{g/R_0}$. Notably, the system's natural frequency $\omega_0 = \sqrt{\omega_C^2 - \omega^2}$ depends on ω, *which is—at the same time—the forcing frequency*.

For $\alpha \neq 0$, we can investigate the oscillations of the bead around the stable equilibrium position $\theta = 0$ to obtain the resonance curve of the forced harmonic oscillator described by equation (10). The maximum angle A_P of the bead as a function of the angular velocity ω is given by [2, 3]

$$\begin{aligned} A_P(\omega) &= \frac{\alpha g}{R_0\sqrt{(\omega_0^2 - \omega^2)^2 + \left(\frac{b}{m}\right)^2\omega^2}} \\ &= \frac{\alpha g}{R_0\sqrt{(2\omega^2 - g/R_0)^2 + \left(\frac{b}{m}\right)^2\omega^2}} \end{aligned} \tag{11}$$

and the maximum value of this function is found at the resonant frequency

$$\omega_P^{\text{res}} = \sqrt{\frac{g}{2R_0} - \frac{b^2}{8m^2}}\,. \tag{12}$$

It is worth noting that this resonance appears as a consequence of the periodic variation of the coefficient of $\cos\theta$ in equation (6).

2.2. Rigid spherical bead and tilted axis of rotation

Here, we consider the fact that the real bead is a rigid steel sphere rolling over the interior groove of the hoop, which has the profile shown in figure 4. This section summarises the relevant results that will be used to compare the model's predictions with the experimental observations. Although not difficult, the exact calculations contain several steps and are

deferred to the appendix. We will show that the formulas for the point-like bead are formally equivalent to the rigid sphere case, but need a nontrivial correction in order to give accurate quantitative predictions.

The EOM for the rigid spherical bead *rolling without slipping* over the interior groove of the hoop is

$$\ddot{\theta} + \kappa\left[\frac{b}{m}\dot{\theta} + \left(\frac{g}{R_{\mathrm{CM}}}\cos\alpha - \omega^2\cos\theta\right)\sin\theta\right] = \kappa\frac{g}{R_{\mathrm{CM}}}\sin\alpha\cos(\omega t)\cos\theta, \tag{13}$$

where

$$\kappa = \left[1 + \gamma\frac{R^2}{R_{\mathrm{CM}}^2}\left(\frac{R_{\mathrm{CM}}}{r} + 1\right)^2\right]^{-1} \tag{14}$$

is a *correction factor* which takes into account the geometric properties of the sphere and the hoop, as well as the sphere's moment of inertia represented by the parameter[1] γ. R_{CM} is the distance from the hoop's centre to the sphere's centre of mass (CM), and r represents the length between the sphere's CM and its instantaneous axis of rotation. The geometrical meaning of each symbol can be inferred from figures 2 and 4.

Analogously to the point-particle case, we can search the values of θ that fulfil the equilibrium condition $\dot{\theta} = \ddot{\theta} = 0$ when $\alpha = 0$ (vertical axis of rotation). Again, $\theta^* = 0$ and $\theta^* = \pi$ are equilibrium positions, but now the critical angular velocity is given by

$$\omega_{\mathrm{C}} = \sqrt{\frac{g}{R_{\mathrm{CM}}}} \tag{15}$$

and when $\omega > \omega_{\mathrm{C}}$ a stable equilibrium position appears

$$\theta^* = \arccos\left(\frac{g}{\omega^2\, R_{\mathrm{CM}}}\right). \tag{16}$$

Despite these differences with respect to the point particle case, the bifurcation diagram is analogous (just changing R_0 by R_{CM}).

Under the assumptions of small angles α and θ, the EOM turns into

$$\ddot{\theta} + \kappa\left[\frac{b}{m}\dot{\theta} + \left(\frac{g}{R_{\mathrm{CM}}} - \omega^2\right)\theta\right] = \kappa\alpha\frac{g}{R_{\mathrm{CM}}}\cos(\omega t). \tag{17}$$

Consequently, the maximum angle reached by the rigid spherical bead as a function of ω is given by

$$A_S(\omega) = \frac{\alpha g}{R_{\mathrm{CM}}\sqrt{\left(\left(\frac{\kappa+1}{\kappa}\right)\omega^2 - \frac{g}{R_{\mathrm{CM}}}\right)^2 + \left(\frac{b}{m}\right)^2\omega^2}} \tag{18}$$

and the angular frequency for maximum amplitude is

$$\omega_S^{\mathrm{res}} = \sqrt{\frac{\kappa}{\kappa+1}\left(\frac{g}{R_{\mathrm{CM}}} - \frac{\kappa}{2(\kappa+1)}\frac{b^2}{m^2}\right)}. \tag{19}$$

It's easy to check that we recover the formulas for the point-particle approximation—equations (5) to (12)—when the correction factor $\kappa = 1$ (which occurs when $\gamma = 0$ or $R = 0$).

[1] The moment of inertia for a sphere is γmR^2, with $\gamma = \frac{2}{5}$. For a cylinder it would be $\gamma = \frac{1}{2}$, for a ring $\gamma = 1$, etc.

Figure 5. Experimental device. The smartphone used to record the motion can be seen at the top of the hoop.

3. Experimental device

In order to test the theoretical models developed in the previous section, we assembled the experimental device shown in figure 5. The construction is straightforward and needs only tools and equipment usually found in teaching laboratories. The whole procedure is accessible to junior students and suitable as a short-term physics project to accompany a vectorial or lagrangian dynamics course.

The device consists of a metallic hoop of radius $R_0 = (0.183 \pm 0.005)$ m with a U-shaped profile (figure 4) of width $L = 0.0174$ m and heigth $a = 0.007$ m, connected to a vertical rotatory axis by means of a 3D printed plastic link (blue part in figure 5). The axis is driven by a belt pulled by a DC motor. The motor and axis are both supported by a cast iron base whose support plane is adjustable by means of two leveling screws, allowing to modify the orientation α of the hoop's rotation axis. The motor is powered by an adjustable current

Figure 6. Camera view from a reference frame fixed to the hoop.

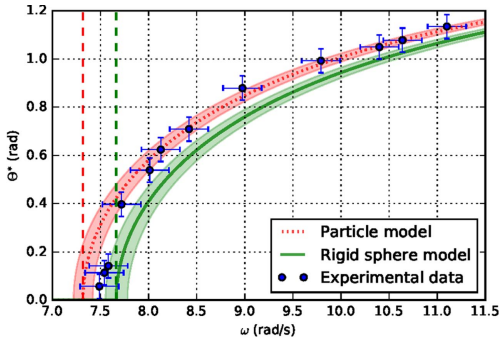

Figure 7. Bifurcation diagram. Comparison between the experimental observations (blue dots), the predictions of the rigid body model (continuous green line) and the particle model (dotted red line). The colour bands represent the uncertainty in the theoretical model due to the experimental error in the parameter R_0. The vertical dashed lines indicate the critical angular velocity predicted by each model.

source which controls the angular velocity of the hoop ω. This velocity is measured using a digital photo-tachometer with an absolute uncertainty of $\Delta\omega = 0.2$ rad s^{-1} (about 2 rpm). The 'bead' is a steel ball with radius $R = (0.0126 \pm 0.0001)$ m and mass $m = (0.066 \pm 0.001)$ kg. The device scheme is shown in figure 2. As was mentioned in the previous section, the groove's profile geometry (shown in figure 4) has to be taken into account to develop an accurate model, because it affects the instantaneous axis of rotation of the sphere and hence the rolling constraint, modifying the EOM.

For tracking the motion of the ball in the moving reference frame of the rotating hoop, a smartphone capable of video recording at 30 fps was fixed to the uppermost point of the hoop using a couple of rubber bands. With this arrangement, the position of the sphere was measured over a metric tape fastened to the interior groove of the hoop, as shown in figure 6. The error estimation for the measured angle was $\Delta\theta = 0.05$ rad (approximately 3°), because the error of the linear distance over the metric tape was estimated as $\Delta x = 0.01$ m. Another camera was used to capture the tachometer reading. After the capture, the two videos were synchronised using the audio track and combined into one, which was analysed to extract the

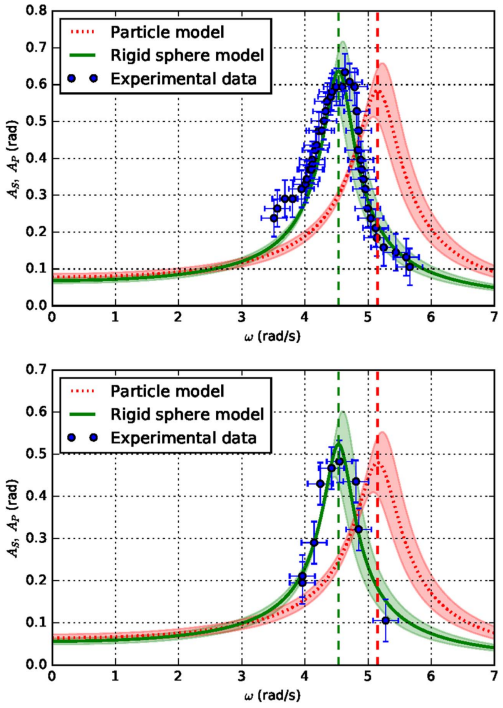

Figure 8. Resonance curves. Comparison between the experimental data, the predictions of the point particle model (equation (11)) and the rigid body model (equation (18)) for a tilt angle $\alpha = 4.5°$ (upper figure) and $\alpha = 3.7°$ (lower figure). The (colour) bands represent the theoretical model uncertainty due to the experimental error in the parameters R_0 and α. The discontinuous vertical lines indicate the resonant frequency for the point particle model (red line, equation (12)) and the rigid sphere model (green line, equation (19)) respectively. The distance between these lines is more than the absolute error of the angular velocity.

needed data—essentially, the ball's position and angular velocity of the hoop[2]. Some videos showing the device at work are available as supplemental material[3].

4. Results and discussion

We empirically tested the predictions of the two models by means of the experimental device and the digital video analysis of the sphere's motion. First, we searched for the bifurcation at the critical angular velocity with the rotation axis perfectly vertical ($\alpha = 0$). Hence we measured the equilibrium angle θ^* as a function of the hoop's angular velocity ω and compared the observed values with the predictions of the particle and rigid sphere models (equations (7) and (16), respectively). We show in figure 7 the results obtained. The predicted critical angular velocities were $\omega_C = 7.3$ rad s^{-1} for the point-particle model and $\omega_C = 7.7$ rad s^{-1} for the rigid sphere model. As can be seen, both models describe well the system's behaviour within the experimental error bounds, so the accuracy gained by using a

[2] This was carried out using the free OpenShot video editing software (http://openshot.org/). However, there are many open source alternatives to accomplish the same purpose.
[3] Supplemental material at http://dx.doi.org/10.5281/zenodo.158943.

more complex model seems to not justify the extra effort, unless we can improve the measurement uncertainty. However, while studying the bifurcation we unexpectedly observed the existence of sustained oscillations of θ around the stable equilibrium point for $\omega < \omega_C$. This observation led to the theoretical analysis of the system's resonance originated in the deviation of the rotation axis of the hoop from the vertical, which was developed in section 2.

The resonant behaviour, appearing when $\omega < \omega_C$ and $\alpha \neq 0$, is exhibited in figure 8, which shows the experimental data obtained for two values of the tilt angle α and the theoretical predictions for both a point particle and a rolling sphere using the actual parameters of the system and its uncertainties. The development of the rigid body model was initially motivated by the systematic discrepancies observed between the empirical data and the prediction of the point particle model. In fact, as can be seen in the figure, the resonance frequency predicted by the point particle model (equation (12)) is $\omega_P^{\text{res}} = 5.2$ rad s^{-1}, while the rigid body model –which also considers the U-shaped profile of the hoop and the resultant rolling constraint–gives a value of $\omega_S^{\text{res}} = 4.5$ rad s^{-1} (as given by equation (19)). Both the resonant frequency and the width of the resonant curve are better described by the rigid sphere model. The difference between both predictions more than doubles the absolute error for the angular velocity measured with the tachometer, which was estimated as $\Delta\omega = 0.2$ rad s^{-1}. There is no way of obtaining the measured resonance frequency from the point particle model by adjusting the friction constant—the only free parameter of the models—which was estimated as $b = 0.09$ kg m^2 s^{-1} and was practically the same for the various tilt angles α considered. This improvement justifies the greater complexity of the rigid sphere model, thereby giving a better account of the empirical data. Raw data (videos and measurements) as well as the Jupyter notebook [9] with the previous calculations and figures can be found at the digital open repository (see footnote 3).

5. Conclusions

Current technology can give new life to old problems. This can be harnessed for the benefit of the students, who can have the chance to smoothly integrate theory and experimental work. In this article, we have shown how this principle can be applied to a particular problem, namely a bead on a rotating hoop, usually found in textbooks as a highly idealised mechanical system. The use of a smartphone's digital camera allowed us to measure the relevant variables of the system from a reference frame fixed to the hoop and to get a quantitative description of the bead's motion in order to compare the predictions of two competing theoretical models. In the past, this has been a difficult operation, hampering the numerical validation of the models and confining the problem within the paper-and-pencil domain.

On the other hand, we improved the experimental determination of the bifurcation diagram and discovered a resonant behaviour that was not previously reported, which occurs when the hoop's rotation axis is not perfectly vertical. This phenomenon is caused by a periodic variation of a parameter present in the EOM due to the uniform rotation of the hoop. We succeeded in accurately describe this behaviour for small values of the tilting angle α.

Overall, we showed that by means of new and readily available technological resources the students can be engaged in a more realistic pathway through the scientific method while learning traditional curriculum topics.

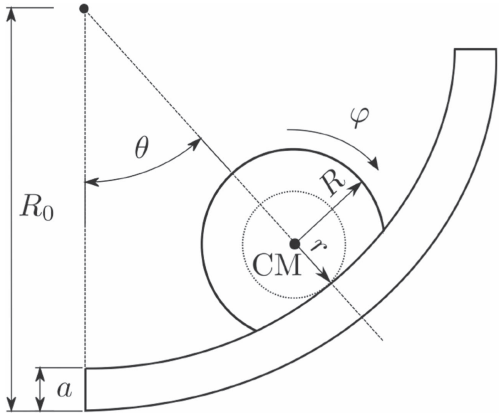

Figure A1. The bead rolling without slipping over the groove.

Acknowledgments

We gratefully acknowledge the Engineering Laboratory at Instituto de Industria and the Physics Laboratory at Instituto de Ciencias for providing physical space, tools and technical support. This work was done under project UNGS–IDEI 30/4077 'Uso de tecnologías de la información y la comunicación como apoyo a la formación de estudiantes de ciencias e ingeniería'.

Appendix

Here we briefly summarise the corrections needed for taking into account the finite size of the bead and the geometry of the hoop's transversal profile, which alter the instantaneous axis of rotation of the bead and hence the EOM. Figure A1 shows the situation. If the sphere turns an angle $\mathrm{d}\varphi$ around its centre while rolling without slipping over the groove, the contact point advances a distance $\mathrm{d}s = r\mathrm{d}\varphi$, where $r = \sqrt{R^2 - L^2/4}$ is the distance between the sphere's centre and the instantaneous axis of rotation (see figure 4). The rolling condition establishes a constraint between θ and φ:

$$\mathrm{d}s = r\ \mathrm{d}\varphi = (R_0 - a)\ \mathrm{d}\theta \Rightarrow \dot{\varphi} = \frac{R_0 - a}{r}\ \dot{\theta}. \tag{20}$$

Meanwhile, the centre of mass of the sphere travels a distance $\mathrm{d}s_{\mathrm{CM}}$ in a reference frame fixed to the hoop,

$$\mathrm{d}s_{\mathrm{CM}} = (R_0 - a - r)\ \mathrm{d}\theta = R_{\mathrm{CM}}\ \mathrm{d}\theta,$$

where $R_{\mathrm{CM}} = R_0 - a - r$ is the distance from the centre of the hoop to the centre of the sphere. Hence the velocity of the centre of mass (relative to the hoop) is

$$v_{\mathrm{CM,rel}} = R_{\mathrm{CM}}\dot{\theta}. \tag{21}$$

The kinetic energy of the sphere is (by Knig's decomposition)

$$\begin{aligned} T &= \frac{1}{2}m(v_{\mathrm{CM,rel}}^2 + (R_{\mathrm{CM}}\sin\theta\ \omega)^2) + \frac{1}{2}I_{\mathrm{CM}}\dot{\varphi}^2 \\ &= \frac{1}{2}mR_{\mathrm{CM}}^2(\dot{\theta}^2 + \omega^2\sin^2\theta) + \frac{1}{2}m\gamma\frac{R^2}{r^2}(R_0 - a)^2\dot{\theta}^2 \\ &= \frac{1}{2}mR_{\mathrm{CM}}^2\left[\left(1 + \gamma\frac{R^2(R_0 - a)^2}{R_{\mathrm{CM}}^2 r^2}\right)\dot{\theta}^2 + \omega^2\sin^2\theta\right] \\ &= \frac{1}{2}mR_{\mathrm{CM}}^2\left(\frac{1}{\kappa}\ \dot{\theta}^2 + \omega^2\sin^2\theta\right), \end{aligned} \tag{22}$$

where $I_{\mathrm{CM}} = \gamma mR^2$ is the sphere's moment of inertia about its centre of mass ($\gamma = 2/5$).

On the other hand, the formula for the potential energy V is analogous to equation (2), just substituting R_0 by R_{CM}. The same substitution applies to formula (4) for the generalised friction force. From the usual operations on the Lagrangian, equation (13) follows.

References

[1] Halloun I A and Hestenes D 1985 Common sense concepts about motion *Am. J. Phys.* **53** 1056
[2] Tipler P A and Mosca G 2008 *Physics for Scientists and Engineers* vol 1 6th edn (New York: Freeman) (see problem 87 on p 167)
[3] Young H D and Freedman R A 2014 *Sears and Zemansky's University Physics: With Modern Physics* vol 1 13th edn (Harlow: Pearson Education) (see problem 5.119 on p 173)
[4] Wilson J D and Hernández-Hall C A 2010 *Physics Laboratory Experiments* 8th edn (Boston, MA: Brooks/Cole)
[5] Kraftmakher Y 2015 *Experiments and Demonstrations in Physics* 2nd edn (Singapore: World Scientific)
[6] Brown D and Cox A J 2009 Innovative uses of video analysis *Phys. Teach.* **47** 145–50
[7] Pearce J M 2014 *Open-Source Lab: How to Build your own Hardware and Reduce Research Costs* (Amsterdam: Elsevier)
[8] Kuhn J 2014 Relevant information about using a mobile phone acceleration sensor in physics experiments *Am. J. Phys.* **82** 94
[9] Pérez F, Granger B E and Hunter J D 2011 Python: an ecosystem for scientific computing *Comput. Sci. Eng.* **13** 13
[10] Taylor J R 2005 *Classical Mechanics* (Herndon, VA: University Science Books) pp 260–4
[11] Strogatz S H 2015 *Nonlinear Dynamics and Chaos* 2nd edn (Boulder, CO: Westview Press)
[12] Sivardière J 1983 A simple mechanical model exhibiting a spontaneous symmetry breaking *Am. J. Phys.* **51** 1016
[13] Drugowich de Felicio J R and Hipólito O 1985 Spontaneous symmetry breaking in a simple mechanical model *Am. J. Phys.* **53** 690
[14] Fletcher G 1997 A mechanical analog of first- and second-order phase transitions *Am. J. Phys.* **65** 74
[15] Ochoa F and Clavijo J 2006 Bead, hoop and spring as a classical spontaneous symmetry breaking problem *Eur. J. Phys.* **27** 1277
[16] Rousseaux G 2007 Bead, hoop and spring...: some theoretical remarks *Eur. J. Phys.* **28** L7–9
[17] Mancuso R V 2000 A working mechanical model for first- and second-order phase transition and the cusp catastrophe *Am. J. Phys.* **68** 271
[18] Mancuso R V and Schreiber G A 2005 An improved apparatus for demonstrating first- and second-order phase transitions: ball bearings on a rotating hoop *Am. J. Phys.* **73** 366
[19] Sungar N *et al* 2001 A laboratory-based nonlinear dynamics course for science and engineering students *Am. J. Phys.* **69** 591
[20] Cross R 2016 Coulomb's law for rolling friction *Am. J. Phys.* **84** 221